GEANT4 for breast dosimetry: parameters optimization study

C Fedon[1,2]**, F Longo**[1,2]**, G Mettivier**[3,4] **and R Longo**[1,2]

. [1] Department of Physics, University of Trieste, Trieste, Italy

. [2] INFN, Sezione di Trieste, Trieste, Italy

. [3] Department of Physics, University of Napoli 'Federico II', Napoli, Italy

. [4] INFN, Sezione di Napoli, Napoli, Italy

E-mail: christian.fedon@ts.infn.it

Abstract

Mean glandular dose (MGD) is the main dosimetric quantity in mammography. MGD evaluation is obtained by multiplying the entrance skin air kerma (ESAK) by normalized glandular dose (DgN) coef cients. While ESAK is an empirical quantity, DgN coef cients can only be estimated with Monte Carlo (MC) methods. Thus, a MC parameters benchmark is needed for effectively evaluating DgN coef cients. GEANT4 is a MC toolkit suitable for medical purposes that offers to the users several computational choices. In this work we investigate the GEANT4 performances testing the main PhysicsLists for medical applications. Four electromagnetic PhysicsLists were implemented: the linear attenuation coef cients were calculated for breast glandularity 0%, 50%, 100% in the energetic range 8–50 keV and DgN coef cients were evaluated. The results were compared with published data. Fit equations for the estimation of the *G*-factor parameter, introduced by the literature for converting the dose delivered in the heterogeneous medium to that in the glandular tissue, are proposed and the application of this parameter interaction-by-interaction or retrospectively is discussed. G4EmLivermorePhysicsList shows the best agreement for the linear attenuation coef cients both with theoretical values and published data. Moreover, excellent correlation factor ($r^2 >$ 0.99) is found for the DgN coef cients with the literature.

The nal goal of this study is to identify, for the rst time, a benchmark of parameters that could be useful for future breast dosimetry studies with GEANT4.

Keywords: breast dosimetry, GEANT4, Monte Carlo code (Some gures may appear in colour only in the online journal)

1. Introduction

Breast cancer is the most common form of the cancer among women worldwide (Malvezzi *et al* 2014, Siegel *et al* 2014) and the breast screening programs are based on x-ray mam- mography. Recently digital breast tomosynthesis (Skaane *et al* 2013) and breast computed tomography (Glick 2007) were proposed to overcome issues related to the low speci city of x-ray mammography due to tissues overlapping in the image. However, the problem of quan- tifying the dose delivered for all these techniques is still a critical issue (Kalender *et al* 2012, Vedantham *et al* 2013).

In mammography, the parameter that quanti es the radiation dose delivered to the glan- dular component of the breast tissue is the mean glandular dose (MGD). The breast consists of different percentages of adipose and glandular tissue: while the adipose tissue is not con- sidered to be at risk of induced cancer, the glandular component is highly radiosensitive. The MGD is calculated from the equation

$$MGD = K_{air} \cdot g \cdot c \cdot s, \quad (1)$$

where K_{air} is the entrance skin air kerma (ESAK) and g, c, s are factors that take into account respectively the air kerma to average glandular dose conversion (as a function of breast thick- ness and the HVL value), the glandularity and the x-ray spectrum (Dance *et al* 2000). These coef cients cannot be estimated with direct measurements and their calculation are only based on computational methods. The Monte Carlo (MC) techniques became the key-instruments to overcome the critical issue of MGD evaluation.

Several authors have intensively used the MC techniques for evaluating these coef cients. The rst authors who investigated this problem, using home-grown softwares, were Kulkarni and Supe (1984), Dance (1990), Dance *et al* (2000, 2009), Dance and Young (2014) and Wu *et al* (1991, 1994). Boone (1999) was the rst to introduce the DgN coef cient (normalized glandular dose) by using generic MC tools for polychromatic spectrum and for monoenergetic beams (Boone 2002).

The use of modern and advanced imaging techniques requires a new de nition of DgN coef cients: the DgN_{CT} coef cients are de ned for cone-beam breast computer tomography by Boone *et al* (2004) and Sechopoulos *et al* (2010), which also described a method for digital tomosynthesis (Sechopoulos *et al* 2006).

GEANT4 is a general-purpose toolkit (Agostinelli *et al* 2003) for MC simulation of par- ticles transport in matter. Different choices of physical processes models are available: users can specify the physical interactions that have to be simulated by implementing the class *G4UserPhysicsList*. Several reference PhysicsLists are routinely validated (Katsuya *et al* 2005) and updated by the GEANT4 collaboration. It is mandatory, for medical applications, to have a very good description of electromagnetic interactions of photons, electrons, hadrons and ions with matter in the energy range of interest. The electromagnetic interactions of pho- tons are crucial for mammographic applications and the choice of the PhysicsList has to be carefully

operated. Even though a large number of dosimetric studies using GEANT4 have been published, there is no information on which is the optimal PhysicsList for breast MC dosimetry.

The choices the researchers make regarding the PhysicsList are not usually stated: sci- enti c papers do not often specify this information (Thacker and Glick 2004, Sechopoulos *et al* 2006, Myronakis *et al* 2013 or Mahdavi *et al* 2015) nor authors make same choices (Lanconelli *et al* 2013, Mittone *et al* 2014 or White *et al* 2014).

In the work reported herein the main four electromagnetic PhysicsList suggested by GEANT4 Low Energy Electromagnetic Physics Working Group for medical purposes

Table 1. Breast tissues composition from Hammerstein *et al* (1979).

Glandularity fraction %	Density (g cm^{-3})	H %	C %	N %	O %	P %
0%	0.9301	11.2	61.9	1.7	25.1	0.1
50%	0.9819	10.7	40.1	2.5	46.4	0.3
100%	1.04	10.2	18.4	3.2	67.7	0.5

(Incerti 2014) are tested by computing the linear attenuation coef cients and by estimating the DgN coef cients; the relative differences are presented and discussed.

The linear attenuation coef cients were computed for broglandular and adipose tissues: the results (in the energy range from 8 keV up to 50 keV) were compared with the data reported in Hammerstein *et al* (1979) and with experimental results of Johns and Yaffe (1987) and Chen *et al* (2010).

The DgN evaluation is carried out introducing *G*-factor coef cient to take into account the glandularity (as described by Wilkinson and Heggie 2001). Even if the use of *G*-factor coef cient is well documented in the literature nevertheless some authors use it interaction- by-interaction (Boone 2002, Thacker and Glick 2004, Sechopoulos *et al* 2006, Myronakis *et al* 2013) while others consider the *G*-factor as an additional coef cient, which has to be added retrospectively for MGD evaluation (Boone 1999, Mittone *et al* 2014). Thus, different results can be achieved: the results of the two approaches (interaction-by-interaction and ret-rospectively) are compared and discussed.

The goal is to give a benchmark (based on MC and experimental results) for the choice of physics modelling out of the possibilities offered in GEANT4 and to highlight the differences among the several choices.

2. Materials and methods

2.1. Geometry, materials and general parameters

Simulations were performed using GEANT4 version 4.10.00 (December 2013). Several runs of point source monochromatic photons within the energy range of 8–50 keV were simulated (with a 1 keV step). The number of primary photons generated was 10^6 and in order to achieve a good statistical uncertainty on the estimated quantities (i.e. a coef cient of variation (COV) less than 0.5%) simulations were repeated using different seeds for each simulation. The monochro- matic photon beam impinged on a slab of one of the selected materials. The thickness was set to 2 cm in order to avoid that all photons were absorbed or traverse the slab without interacting. The target was lled by homogeneous breast tissue of different glandularity: the composition used was that one proposed by Hammerstein *et al* (1979) and shows in table 1.

2.1.1. PhysicsList.
A brief description of the electromagnetic PhysicsLists suitable for medi- cal applications is provided by the GEANT4 Low Energy Electromagnetic Physics Working Group (Incerti 2014) and it is summarized in table 2.

The list in table 2 is not comprehensive: other PhysicsLists are available but they do not substantially differ from the PhysicsLists mentioned in table 2 (e.g. G4EmLivermorePolarizedPhysics or G4EmEPPhysics) or they are not suitable for breast dosimetry (e.g. G4EmDNAPhysics).

The four PhysicsLists were separately implemented in the MC code: the performances were tested by calculating the linear attenuation coef cient and by estimating the DgN coef cients.

Table 2. PhysicsLists suitable for medical applications (Incerti 2014).

PhysicsLists	Characteristics
G4EmStandardPhysics	Standard EM Physics
G4EmLivermorePhysics	Low energy EM physics using Livermore data
G4EmStandardPhysics-Option4	Most accurate physics models from standard and low energy
G4EmPenelopePhysics	Low energy EM implementing Penelope models

2.2. Linear attenuation coefficient

The linear attenuation coef cient (μ) was obtained using the following formula:

$$\mu = \frac{-\ln\left(\frac{I_{\text{out}}}{I_0}\right)}{x}, \tag{2}$$

where I_{out} is the number of primary photons going out from the box sample, I_0 is the number of photons entering the volume and x is the thickness of phantom. When a photon has an interaction, the simulation's event is aborted. Data were stored in appropriate variables that allowed us to calculate the coefficients.

The results were rstly compared with the data provided in Hammerstein *et al* (1979) and then with the experimental results of Johns and Yaffe (1987) and Chen *et al* (2010) by using the relative difference *R%*:

$$R\% = \frac{\mu - \mu^*}{\mu^*} \times 100, \tag{3}$$

where μ is the linear attenuation coef cient calculated in the present work and μ^* is the linear attenuation coef cient presented in Hammerstein *et al* (1979) or the experimental one.

2.3. G-factor

The *G*-factor is a parameter introduced by Boone (1999) for estimating the DgN that quanti- es the energy absorbed by only the glandular fraction of the breast. It is calculated as follows:

$$G = \frac{f_g \left(\frac{\mu_{en}}{\rho}\right)_g}{\left[f_g \left(\frac{\mu_{en}}{\rho}\right)_g + (1 - f_g)\left(\frac{\mu_{en}}{\rho}\right)_a\right]}, \tag{4}$$

where the mass energy absorption coef cients (μ_{en}/ϱ) are referred with an *a* subscript for adipose tissue and with a *g* subscript for glandular tissue, while f_g is the glandular fraction, by weight, of the breast tissue ($f_g = 1$ for glandular, $f_g = 0.5$ for 50% glandular etc).

In this work the *G*-factor implementation is compared for two scenarios: (i) it is added retrospectively, when $(\mu_{en}/\varrho)_a$ and $(\mu_{en}/\varrho)_g$ are related to the beam primary energy, (ii) it is estimated interaction-by-interaction. The method proposed by Okunade (2007) was used for calculating the mass energy absorption coef cient for all the compounds elements; according to that method values of $(\mu_{en}/\varrho)_a$ or $(\mu_{en}/\varrho)_g$ were obtained as follows:
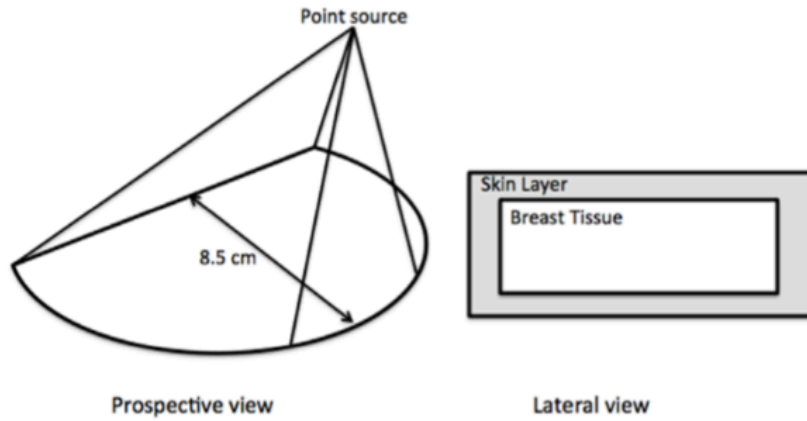
Figure 1. Schematic representation of the simulated geometry: the prospective view (on the left side) shows the semi-cylindrical breast shape and the x-ray point source; the lateral view (on the right side) shows the skin layer and the inner homogeneous breast tissue.

$$\left(\frac{\mu_{en}}{\rho}\right)_a = \sum_i W_i\left[\frac{\mu_{en}}{\rho}(x)\right]_i \text{ or } \left(\frac{\mu_{en}}{\rho}\right)_g = \sum_i W_i\left[\frac{\mu_{en}}{\rho}(x)\right]_i, \tag{5}$$

where $[(\mu_{en}/\rho)(x)]_i$ are the mass energy absorption coefﬁcients for the ith element and W_i is the fraction by weight for the ith element in the compound.

Values of $(\mu_{en}/\rho)_a$ and $(\mu_{en}/\rho)_g$ obtained by (5) were ﬁtted in the interval energy 8–50 keV using the ROOT Data Analysis Framework (2014).

2.4. DgN coefficients

The geometry of the DgN coefﬁcients calculation is comprehensively described in the work of Boone (2002), whilst here only an outline is given. A semi-cylindrical breast shape was simulated (with a thickness ranging from 2 to 9 cm with a 1 cm step) with a radius of 8.5 cm and a skin layer of 0.4 cm (ﬁgure 1). A semi-cone shaped radiation ﬁeld irradiated the breast (with energy from 8 up to 50 keV with a 1 keV step) from a ﬁxed distant of 65 cm. The breast homogeneous tissue composition is shown in table 1.

For each breast thickness and breast composition, the number of monochromatic primary photons generated was 10^6 and simulations were repeated nine times (per each case), using different seeds, for achieving a COV value less than 0.5%. The MGD, in mGy, was obtained as follows:

$$MGD = \frac{E_{dep} \cdot G}{mass_g \cdot f_g}, \tag{6}$$

where E_{dep} is the energy delivered to the breast tissue (without skin), G is the G-factor as in equation (4), $mass_g$ is the mass of the breast (without skin), f_g is the glandular fraction. DgNs were then calculated as following:

$$DgN(E) = \frac{MGD}{\chi},$$

(7)

Where χ is the exposure (in Röntgen) at the surface of irradiated breast.
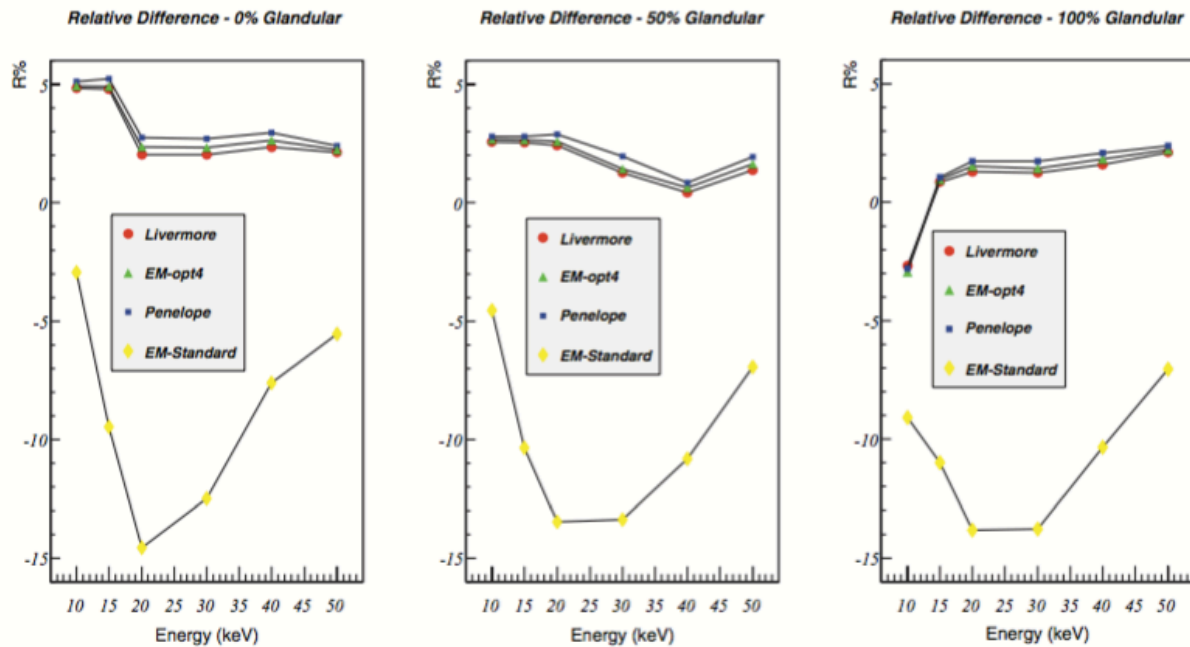

Figure 2. $R\%$ values for 0% (left side), 50% (centre) and 100% (right side) glandular fraction. All graphs show the comparison between G4EmLivermorePhysics (red dots), G4EmStandardPhysics-Option4 (green triangles), G4EmPenelopePhysics (blue squares) and G4EmStandardPhysics (yellow diamonds) as a function of energy.

PhysicsLists were implemented in the MC code and Wilcoxon Signed Rank test was used on simulated data for a statistic comparison with the results obtained by Boone (2002).

3. Results and discussion

3.1. Linear attenuation coefficient analysis

The relative difference $R\%$ (equation (3)) for the G4EmStandardPhysics is in the range of 3–14.5% while for the three low energy PhysicsLists is within range of 0.5–5.2% (gure 2): among them the best results are always obtained by G4EmLivermorePhysics.

G4EmStandardPhysics can be considered as a starting point of every GEANT4 simulation: the Rayleigh effect is not available in the G4EmStandardPhysics and the set of models for the particles interactions are different from three low energy PhysicsLists (Katsuya *et al* 2005).

Figure 3 focuses the attention on G4EmLivermorePhysics (i.e. the PhysicsList that obtained the best results, gure 2) and reports the comparison with Hammerstein *et al* (1979) and experimental values obtained by Johns and Yaffe (1987) and Chen *et al* (2010).

A good agreement is found for the 100% glandular tissue: maximum difference of 2.7% with data of Hammerstein *et al* (1979) and maximum difference of 2.6% with experimental data (Johns and Yaffe 1987). Larger differences are observed for the 0% glandular at the low energies: maximum difference of 4.8% with data of Hammerstein *et al* (1979) and maxi- mum overestimation of 10% with experimental data (Johns and Yaffe 1987). The agreement between simulated data and Hammerstein *et al* (1979) was expected as both glandular and adi- pose tissues composition is the same (see table 1). The experimental linear attenuation coef- cients of the adipose tissues are lower that the MC data; however, the fat values of the two experimental data set (of Johns and Yaffe 1987 and Chen *et al* 2010) are comparable within the experimental uncertainties. The differences with MC data decrease at the high energies, up to be negligible at 50 keV. Such a systematic overestimation of the adipose linear attenuation coef cients based on Hammerstein data can be related to experimental uncertainties of the fat composition or density and to the inter-individual variability (Pani *et al* 2004).
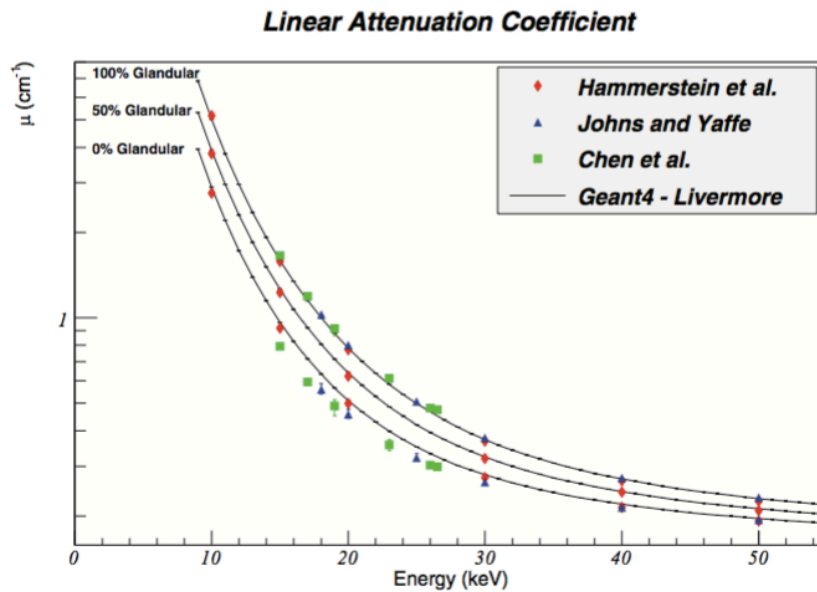

Figure 3. Linear attenuation coefficient obtained using G4EmLivermorePhysics for 0%–50%–100% glandular fraction (solid lines). Data obtained by Hammerstein *et al* (1979) are reported by red diamonds, experimental results of Johns and Jaffe (1987) are shown by blue triangles, while Chen *et al* (2010) are shown by green squares. The bars on experimental data refer to the values range.

3.2. G-factor analysis

The $(\mu_{en}/\varrho)_a$ and $(\mu_{en}/\varrho)_g$ evaluations, obtained using equation (5), are presented in gure 4: the t functions are composed by several parts, which best- tted speci c energy interval. All t functions show an excellent correlation ($r^2 > 0.999$) with the NIST data (a difference below 0.1% was achieved). Wilcoxon Signed Rank test was used between NIST data and t data: t data were not signi cantly different from the NIST data (p-value for adipose 0.98; p-value for glandular 0.99).

Tables 3 and 4 report the mathematical equations and the related parameters of t functions.

After implementing the proposed t equations inside the MC program, the G-factor analy- sis was carried on according to equations (4) and (6).

Figure 5 shows the results of applying the G-factor interaction-by-interaction (solid line) or retrospectively (dotted line) for a 50% glandular breast using G4EmLivermorePhysics (simi- lar behaviour is found for all other glandular fractions).

The retrospectively G-factor application leads to an overestimation of MGD of 7% (at 10 keV) that decreases with the energy increase: at 10 keV the linear attenuation coef cient of several tissues is higher than a high energy. The low energy photons (10 keV) were mainly attenuated by the skin layer (Boone 1999) causing an energy reduction of the incoming photon. Thus higher values for $(\mu_{en}/\varrho)_a$ and $(\mu_{en}/\varrho)_g$ are applied for the G-factor glandular calculation.

The effect of skin attenuation decreased while increasing the energy (20 keV) but pho- tons were also attenuated by breast material. In fact, at this energy, the photoelectric effect is predominant and the energy delivered to the tissue is the highest possible (gure 6). At 50 keV the tissue attenuation is lower, so the G-factor applied interaction-by-interaction is almost equal to the one applied retrospectively (due also to the smoother trend of energy absorption coef cients).
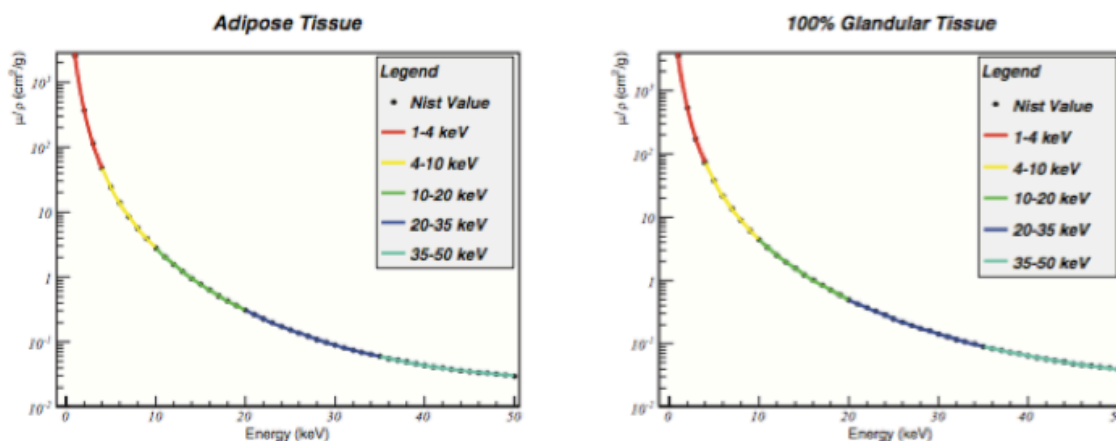

Figure 4. NIST values of mass energy absorption coefficient (black dots) and fit functions (with different colours).

Table 3. Fit functions and parameters values for $(\mu_{en}/\rho)_a$.

Energy range (keV)	Fit equation	Parameters value
1–4	$(a/(x^b + c)) + d$	$a = 2768.13\ b = 2.880\,37\ c = 0.073\,67\ d = -3.239\,78$
4–10	$(a/(b + c \cdot x^d)) + e$	$a = 507\,07.5\ b = 13.9004\ c = 14.5793\ d = 3.082\,51$ $e = -0.089\,153$
10–20	$(a/(b + c \cdot x^3)) + d + e \cdot x$	$a = 559\,66.6\ b = -580.838\ c = 20.0272\ d = -0.145\,142$ $e = 0.005\,073\,72$
20–35	$(a/(b + c \cdot x^3)) + d + e \cdot x$	$a = 43.9956\ b = -11.1528\ c = 0.019\,2767\ d = -0.008\,92$ $e = 0.000\,4033$
35–50	$(a/(b + c \cdot x^3)) + d$	$a = 2.6947 \times 10^6\ b = -1.4991 \times 10^7\ c = 1847.76$ $d = 0.017\,5524$

Table 4. Fit functions and parameters values for $(\mu_{en}/\rho)_g$.

Energy range (keV)	Fit equation	Parameters value
1–4	$(a/(x^b + c)) + d$	$a = 3664.9\ b = 2.7337\ c = 0.009\,753\ d = -9.015\,74$
4–10	$(a/(b + c \cdot x^d)) + e$	$a = 732\,26.7\ b = 17.6474\ c = 14.2058\ d = 3.0487$ $e = -0.140\,218$
10–20	$(a/(b + c \cdot x^3)) + d + e \cdot x$	$a = 892\,136\ b = -4276.73\ c = 198.54\ d = -0.200\,05$ $e = 0.006\,7657$
20–35	$(a/(b + c \cdot x^3)) + d + e \cdot x$	$a = 73.0777\ b = -5.986\,09\ c = 0.018\,57\ d = -0.032\,48$ $e = 0.000\,8786$
35–50	$(a/(b + c \cdot x^3)) + d$	$a = 5.0999\ b = -10.7473\ c = 0.018\,41\ d = 0.016\,17$

The retrospective application of *G*-factor leads to the scenario in which an incorrect glan- dular weighting factor is applied to the total energy deposited: the energy reduction, due to the skin layer and glandular material, is not further taken into account thus, the values for $(\mu_{en}/\varrho)_a$ and $(\mu_{en}/\varrho)_g$ are always lower, leading to a higher *G*-factor.
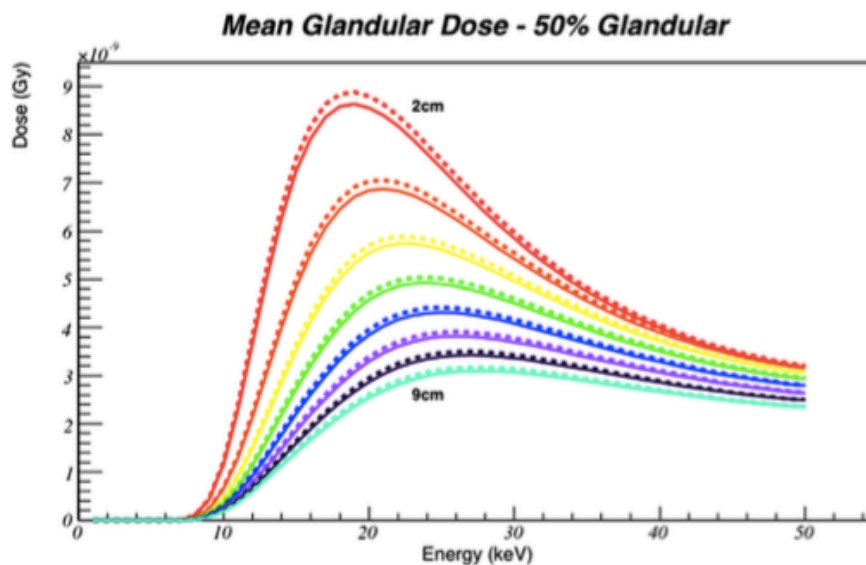

Figure 5. *G*-factor applied interaction by interaction (solid line) and retrospectively (dotted line) as a function of monochromatic energy. The data are shown for breast thickness ranging from 2 up to 9 cm.
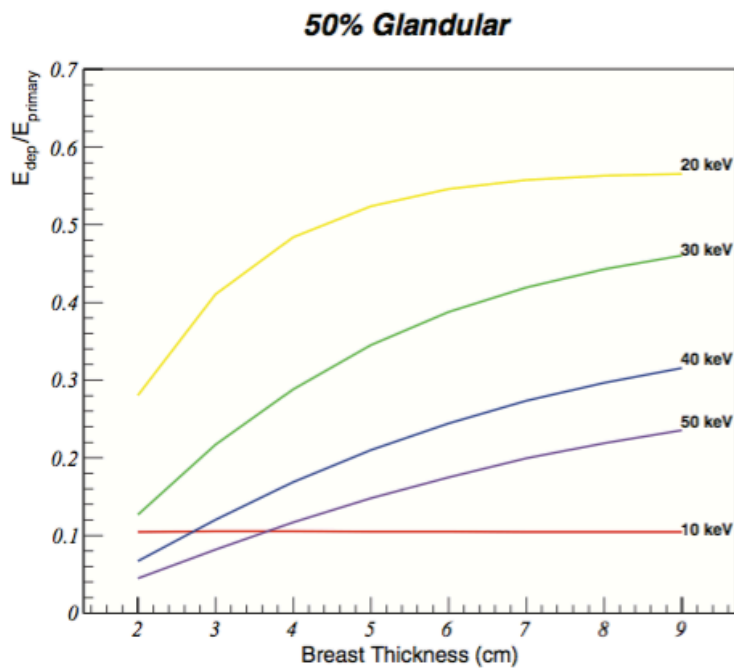
Figure 6. Ratio between the energy delivered to the glandular tissue and the primary energy as a function of breast thickness: for low energy (10 keV) the skin layer effect is constant for all thicknesses while the increase of the primary energy leads to a decrease of energy delivered (after 20 keV).

3.3. DgN analysis

The DgN analysis presented in this section is limited to the *standard breast*: as de ned in the European Guidelines (2006) the standard breast consists of a 4 cm central region of a mixture of adipose and glandular tissue surrounded by a 0.5 cm of adipose layer.

Figure 7 shows the comparison between the four PhysicsLists tested and the data of Boone (2002) for a standard breast. G4EmStandardPhysics (yellow diamonds) shows the larger difference (up to 6%), G4EmStandardPhysics-Option4 and G4EmPenelopePhysics have similar behaviour (with maximum difference of 2%) while the best agreement (with difference close to 1%) is observed for G4EmLivermorePhysics. Thus, an underestimation of the DgN coef- cient leads to an underestimation of the MGD (e.g. when using G4EmStandardPhysics).

Regression line analysis for the G4EmLivermorePhysics shows an excellent agreement between the simulated data (obtained by GEANT4) and Boone (2002) work (gure 8).

Notwithstanding, same analyses were performed for all the breast thicknesses, glandu- lar compositions and PhysicsLists. Due to space limitations, these results are summarized in table 5 through the p-value obtained by the Wilcoxon Signed Rank test applied to the thinner (2cm) and larger (9cm) breast thickness. The best agreement with Boone (2002) data are obtained with G4EmLivermorePhysics PhysicsList (p-value range 0.84–0.99) while the worst is observed with G4EmStandardPhysics PhysicsList (p-value range 0.10–0.79).

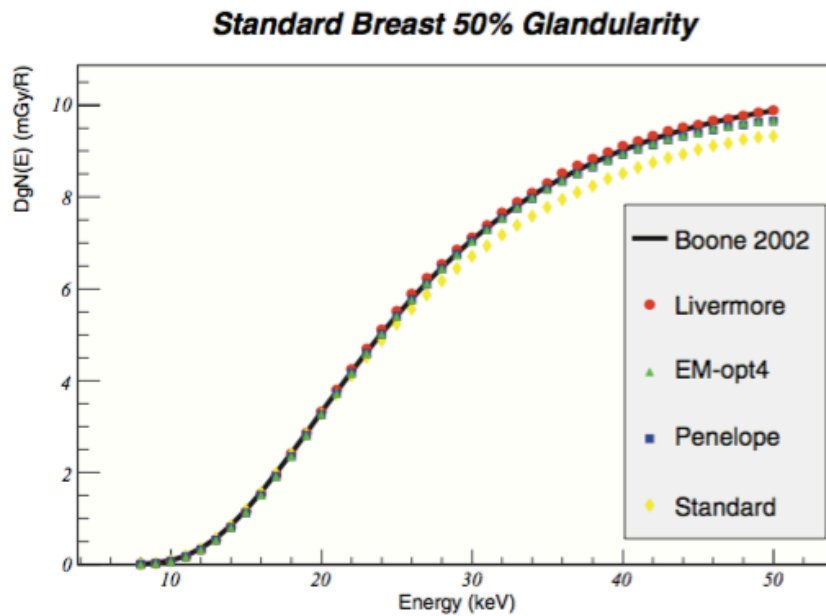**Standard Breast 50% Glandularity**

Figure 7. Comparison of DgN values for the Boone (2002) data (black solid line) against the computed data for the different PhysicsLists: G4EmLivermorePhysics (red dots), G4EmStandardPhysics-Option4 (green triangles), G4EmPenelopePhysics (blue squares) and G4EmStandardPhysics (yellow diamonds).

3.3. DgN analysis

The DgN analysis presented in this section is limited to the *standard breast*: as de ned in the European Guidelines (2006) the standard breast consists of a 4 cm central region of a mixture of adipose and glandular tissue surrounded by a 0.5 cm of adipose layer.

Figure 7 shows the comparison between the four PhysicsLists tested and the data of Boone (2002) for a standard breast. G4EmStandardPhysics (yellow diamonds) shows the larger difference (up to 6%), G4EmStandardPhysics-Option4 and G4EmPenelopePhysics have similar behaviour (with maximum difference of 2%) while the best agreement (with difference close to 1%) is observed for G4EmLivermorePhysics. Thus, an underestimation of the DgN coef- cient leads to an underestimation of the MGD (e.g. when using G4EmStandardPhysics).

Regression line analysis for the G4EmLivermorePhysics shows an excellent agreement between the simulated data (obtained by GEANT4) and Boone (2002) work (figure 8).

Notwithstanding, same analyses were performed for all the breast thicknesses, glandu- lar compositions and PhysicsLists. Due to space limitations, these results are summarized in table 5 through the *p*-value obtained by the Wilcoxon Signed Rank test applied to the thinner (2cm) and larger (9cm) breast thickness. The best agreement with Boone (2002) data are obtained with G4EmLivermorePhysics PhysicsList (*p*-value range 0.84–0.99) while the worst is observed with G4EmStandardPhysics PhysicsList (*p*-value range 0.10–0.79).
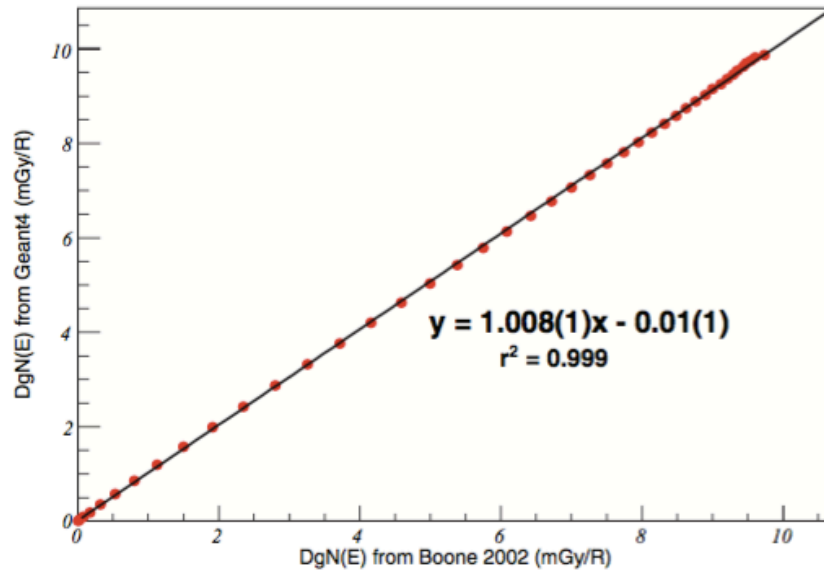
Figure 8. Regression fit line between Boone (2002) data (abscissa) and simulated data (ordinate) by using G4EmLivermorePhysics: an excellent agreement is found. The uncertainty on the last digit is 1 for both the slope and the intercept value.

Table 5. *P*-value results of the Wilcoxon Signed Rank applied to the MC outcomes (for the different PhysicsLists) and Boone (2002) data.

Thickness PhysicsList	2 cm	9 cm
0% Glandular composition		
G4EmLivermorePhysics	0.89	0.98
G4EmStandardPhysics-Option4	0.67	0.61
G4EmPenelopePhysics	0.71	0.62
G4EmStandardPhysics	0.10	0.44
50% Glandular composition		
G4EmLivermorePhysics	0.97	0.98
G4EmStandardPhysics-Option4	0.83	0.85
G4EmPenelopePhysics	0.62	0.74
G4EmStandardPhysics	0.20	0.61
100% Glandular Composition		
G4EmLivermorePhysics	0.99	0.84
G4EmStandardPhysics-Option4	0.49	0.66
G4EmPenelopePhysics	0.47	0.66
G4EmStandardPhysics	0.25	0.79

4. Conclusions

The aim of this study is the optimization of GEANT4 MC parameters for breast dosimetry. A comparison among the main four PhysicsLists for medical applications (Incerti 2014) was carried out based on the evaluation of the linear attenuation coef cients for breast tissues and based on the DgN coefficients.

The G4EmLivermorePhysics PhysicsList shows the best results: a good agreement between MC output and experimental data is found for the linear attenuation coef cient, while an excellent agreement (r^2 = 0.999) is found for the DgN coef cient comparison. Thus, the G4EmLivermorePhysics PhysicsList allows an accurate evaluation of MGD. Moreover, according to our experience, the G4EmStandardPhysics PhysicsList leads to an underestimation of MGD and should not be used for breast dosimetry.

Another source of error is the retrospective use of the *G*-factor glandular coef cient for the evaluation of MGD, instead of interaction-by-interaction. In the former the value is higher causing an overestimation on the MGD up to 7%.

The differences among the three low energy PhysicsLists, tested in this work, can be considered small if compared to other assumption commonly used for the MGD evaluation (e.g. glandular composition of the breast, homogeneity of breast material etc.) however, in order to compare different MC results, the applied PhysicsLists should be clearly stated.

References

Agostinelli S *et al* 2003 Geant4—a simulation toolkit *Nucl. Instrum. Methods* A **506** 250–303

Boone J M 1999 Glandular breast dose for monoenergetic and high-energy x-ray beams: Monte Carlo assessment *Radiology* **213** 23–37

Boone J M 2002 Normalized glandular dose (DgN) coefficients for arbitrary x-ray spectra in mammography: computer-fit values of Monte Carlo derived data *Med. Phys.* **29** 869–75

Boone J M, Shah N and Nelson T R 2004 A comprehensive analysis of DgNCT coefficients for pendant-geometry cone-beam breast computed tomography *Med. Phys.* **31** 226–35

Chen R C *et al* 2010 Measurement of the linear attenuation coefficients of breast tissue by synchrotron radiation computed tomography *Phys. Med. Biol.* **55** 4993–5005

Dance D R 1990 Monte-Carlo calculation of conversion factors for the estimation of mean glandular breast dose *Phys. Med. Biol.* **35** 1211–20

Dance D R, Skinner C L, Young K C, Beckett J R and Kotre C J 2000 Additional factors for the estimations of mean glandular breast dose using the UK mammography dosimetry protocol *Phys. Med. Biol.* **45** 3225–40

Dance D R and Young K C 2014 Estimation of mean glandular dose for contrast enhanced digital mammography: factors for use with the UK, European and IAEA breast dosimetry protocols *Phys. Med. Biol.* **59** 2127–37

Dance D R, Young K C and van Engen R E 2009 Further factors for the estimation of mean glandular dose using the United Kingdom European and IAEA breast dosimetry protocols *Phys. Med. Biol.* **54** 4361–72

European Commission 2006 *European Guidelines for Quality Assurance in Breast Cancer Screening and Diagnosis* 4th edn (Luxembourg: Office for Official Publications of the European Communities)

Glick S J and Breast C T 2007 *Annu. Rev. Biomed. Eng.* **9** 501–26

Hammerstein G R, Miller D W, White D R, Masterson M E, Woodard H Q and Laughlin J S 1979 Absorbed radiation dose in mammography *Radiology* **130** 485–91

Incerti S 2014 for the GEANT4 Low energy electromagnetic physics working group (https://twiki.cern.ch/twiki/bin/view/Geant4/LowePhysicsLists)

Johns P C and Yaffe M J 1987 X-ray characterization of normal and neoplastic breast tissues *Phys. Med. Biol.* **32** 675–95

Kalender W A, Beister M, Boone J M, Kolditz D, Vollmar S V and Weigel M C C 2012 High-resolution spiral CT of the breast at very low dose: concept and feasibility consideration *Eur. Radiol.* **22** 1–8

Katsuya A *et al* 2005 Comparison of Geant4 electromagnetic physics models against the NIST reference data *IEEE Trans. Nucl. Sci.* **52** 910–8

Kulkarni R N and Supe S J 1984 Radiation dose to the breast during mammography: a comprehensive, realistic Monte Carlo calculation *Phys. Med. Biol.* **29** 1257–64

Lanconelli N, Mettivier G, Lo Meo S and Russo P C 2013 Investigation of the dose distribution for a cone beam CT system dedicated to breast imaging *Phys. Med.* **29** 379–87

Mahdavi S R, Esmaeeli A D, Pouladian M, Monfared A S, Sardari D and Bagheri S 2015 Breast dosimetry in transverse and longitudinal field MRI-Linac radiotherapy system *Med. Phys.* **42** 925–36

Malvezzi M, Bertuccio P, Levi F, La Vecchia C and Negri E 2014 European cancer mortality prediction for the year 2014 *Ann. Oncol.* 1–7

Mittone A, Bravin A and Coan P 2014 Radiation dose in breast CT imaging with monochromatic x-rays: simulation study of the influence of energy, composition and thickness *Phys. Med. Biol.* **59** 2199–217

Myronakis M E, Zvelebil M and Darambara D G 2013 Normalized mean glandular dose computation from mammography using GATE: a validation study *Phys. Med. Biol.* **58** 2247–65

Okunade A 2007 Parameters and computer software for the evaluation of mass attenuation and mass energy-absorption coefficients for body tissues and substitutes *J. Med. Phys.* **32** 124–32

Pani S *et al* 2004 Breast tomography with synchrotron radiation: preliminary results *Phys. Med. Biol.* **49** 1739–54

ROOT Data Analysis Framework 2014 (http://root.cern.ch/drupal/)

Sechopoulos I, Si Jia Feng S and D'Orsi Carl J 2010 Dosimetric characterization of a dedicated breast computed tomography clinical prototype *Med. Phys.* **37** 4110–20

Sechopoulos I, Suryanarayanan S, Vedantham S, D'Orsi Carl J and Karellas A 2006 Computation of the glandular radiation dose in digital tomosynthesis of the breast *Med. Phys.* **34** 221–32

Siegel R, Ma J, Zou Z and Jernel A 2014 Cancer statistics *CA Cancer J. Clin.* **64** 9–29

Skaane P *et al* 2013 Comparison of digital mammography alone and digital mammography plus tomosynthesis in a population-based screening program *Radiology* **267** 1

Thacker S C and Glick S J 2004 Normalized glandular dose (DgN) coefficients for flat-panel CT breast imaging *Phys. Med. Biol.* **49** 5433–44

Vedantham S, Shi L, Karellas A, O'Connell A M and Conover D L 2013 Personalized estimates of radiation dose from dedicated breast CT in a diagnostic population and comparison with diagnostic mammography *Phys. Med. Biol.* **58** 7921–36

Wilkinson L and Heggie J 2001 Glandular breast dose: potential errors *Radiology* **213** 1

White S A, Landry G, Fonseca G P, Holt R, Rusch T, Beaulieu L, Verhaegen F and Reniers B 2014 Comparison of TG-43 and TG-186 in breast irradiation using a low energy electronic brachytherapy *Med. Phys.* **41** 061701

Wu X, Barnes G T and Tucker D M 1991 Spectral dependence of glandular tissue dose in screen-film mammography *Radiology* **179** 143–8

Wu X, Gingold E L, Barnes G T and Tucker D M 1994 Normalized average glandular dose in molybdenum target-rhodium filter and rhodium filter mammography *Radiology* **193** 83–9